

EFFECT OF THE REACTION CONDITIONS ON AL-PILLARED MONTMORILLONITE SUPPORTED COBALT-BASED CATALYSTS FOR FISCHER TROPSCH SYNTHESIS

N. AHMAD^{a,b*}, S.T. HUSSAIN^b, B. MUHAMMAD^a, T. MAHMOOD^b, Z. ALI^{b,d},
N. ALI^c, S.M. ABBAS^b, R. HUSSAIN^b, S.M. ASLAM^e

^a Department of Chemistry, Hazara University, Mansehra, Pakistan.

^b National Centre for Physics, QAU campus, Islamabad, Pakistan.

^c Department of Physics, University of the Punjab, Lahore, Pakistan.

^d CEES, University of the Punjab, Lahore, Pakistan.

^e Department of Physics, KUST, Kohat, Pakistan.

Fischer-Tropsch (FT) synthesis in fixed bed micro reactor (high pressure reaction cell) was studied over different wt% Co supported Na-montmorillonite (NaMMT) and Al-pillared montmorillonite (AIMMT) catalysts. The synthesized catalysts were characterized by XRD, TPR, NH₃-TPD, TGA, BET and SEM techniques. FT reaction was carried out at temperature 225, 260 and 275 °C and pressure of 1, 5, and 10 bar. Co supported NaMMT catalysts showed very lower CO-conversion along with increase methane selectivity while AIMMT supported Co catalysts gave higher CO-conversion and lower methane selectivity. With increase in reaction temperature from 225 °C to 275 °C methane selectivity and CO-conversion increased and the selectivity towards C₅₊ hydrocarbons decreased. Decrease in methane selectivity while increase in C₅₊ hydrocarbons and CO-conversion was observed when the pressure was increased to 5 and 10 bar.

(Received January 8, 2013; Accepted February 8, 2013)

Keywords: Pillared montmorillonite, Aluminium, Cobalt, FT Synthesis, Catalysis, Coal gasification

1. Introduction

Due to the increasing energy demand and rapidly depleting resources of petroleum, huge reservoir of natural gas, coal and biomass can be utilized as an alternative to crude oil for the synthesis of sulfur, aromatics and nitrogen free ultra clean fuel along with value added fine chemicals via Fischer-Tropsch (FT) synthesis [1,2]. FT synthesis reaction has attracted worldwide attention to convert syngas (CO and H₂) via gasification of coal, natural gas and biomass to liquid hydrocarbons by the use of different catalysts [3,4].

The most widely used catalysts for the FT synthesis include different forms of Ni, Fe, Ru and Co metals [5]. The use of these catalysts is limited due to the excessive CH₄ production in case of Ni and high price of Ru, leaving only Co and Fe as feasible catalysts in FT synthesis [6]. Due to the lower extent of deactivation, water gas shift activity and selectivity towards linear hydrocarbons, Co is preferred over Fe-based catalysts in academic as well as on industrial scale [7].

The choice of support plays a significant role in FT synthesis, the activity and product selectivity of catalysts is markedly affected by the nature of support [8]. A variety of supports such as SiO₂, Al₂O₃, SBA-15, MCM 48 have been used to improve the dispersion of Co hence its catalytic activity [9-13].

*Corresponding author: nisar_shawar@yahoo.com, nisarchemist@gmail.com

In FT synthesis, Zeolites have been used as a support to synthesize hydrocarbons of specific molecular weights and to change the FT catalyst products distribution. The use of montmorillonite (MMT) as a support for iron based FT catalyst and for the catalysts used in hydrocracking of petroleum have been extensively studied [14]. But the main problem associated with the MMT supported FT catalysts is the production of large amount of methane and carbon dioxide, which are thought to be the most unwanted products in FT synthesis and must be reduced to the minimum possible levels. The production of large amount of methane and carbon dioxide was attributed to hindered reduction of metal oxide to metallic state by sodium montmorillonite (NaMMT) [9]. Beside this, the presence of alkali and alkaline earth metals specially Na showed marked negative effect on activity of FT catalysts due to the inhibition of metal oxide reduction [2]. Sodium ions and calcium ions present between the layers of minerals clay MMT can balance the net negative charge on the lattice produced by the substitution of Si^{4+} with Al^{3+} and Al^{3+} with Mg^{2+} due to which the MMT governs the property to grip guest molecules between its layers. Pillaring agent such as hydroxy-metal cations can be used for the separation or support of MMT lattice layers by replacing the alkali metals and alkaline earth metals cations which upon calcinations results into the formation of large surface area microporous material. To obtain high surface area and pore volume, different metal oxides e.g. oxide of Al, Ti, Zr, and Cr have been used to replace the sodium ion present in the interlayer of MMT clay [15].

It is reported by different investigators that increase in acidic properties as well as texture modification of clay can be achieved when the clay is exchanged with different cations. MMT clays shows efficient catalytic activity towards liquid phase organic synthesis [14]. The pillaring of NaMMT with Al enhances the surface area of support MMT. It also increases the pore volume and pore diameter due to the contribution of Al to replace the Na^+ present in the interlayer of MMT [2].

The use of Co catalysts for lower temperature FT synthesis has attracted worldwide attention. But after a long run of reaction the catalytic activity of cobalt-based FT catalysts become lowered which was attributed to the formation of higher molecular weight hydrocarbons (waxes) responsible for the blocking of active sites of catalysts.

The aim of present study was to convert these waxes during FT synthesis to lower hydrocarbons by the use of MMT (acidic support) supported Co-based FT catalysts. So far the application of pillared MMT catalysts is mainly concerned with the hydrocracking of petroleum products in refineries and there are very limited reports on the application of Co supported MMT catalysts in FT synthesis. The effect of reaction temperature, pressure and reactant gas flow is not reported yet.

2. Experimental

2.1 Materials

NaMMT, aluminium chloride ($\text{AlCl}_3 \cdot 6\text{H}_2\text{O}$) and cobalt nitrate ($\text{Co}(\text{NO}_3)_2 \cdot 6\text{H}_2\text{O}$) from Sigma Aldrich were of analytical grade and were used without any further purification. NaMMT was selected as a starting material to prepare the AlMMT.

2.2 Preparation of AlMMT

In the typical synthesis procedure, 0.5 M NaOH solution was slowly added to 0.25 M solution of $\text{AlCl}_3 \cdot 6\text{H}_2\text{O}$ with OH/Al ratio of 2/1 with continuous stirring. The above suspension was aged at room temperature for 24 h. In the second step, above pillaring solution was added (5 mmol Al/g of clay) to the suspension of 2wt% MMT and stirred for three hour at 100 °C. The resultant slurry was centrifuged at 5000 rpm, washed several times with deionized water in order to remove excess sodium and chlorine, dried at 100 °C overnight, grinded and finally calcined at 400 °C for 5 h [16,17].

2.3 Preparation of 10, 15, 20, 25wt% Co/AlMMT

Wet impregnation method was adopted to synthesize AlMMT catalyst containing 10,15, 20 and 25wt% Co. To prepare 5g of catalyst 4.5, 4.25, 4 and 3.75g of calcined pillared clay was added to 0.1 M solution of $\text{Co}(\text{NO}_3)_2 \cdot 6\text{H}_2\text{O}$ (2.46, 3.69, 4.92 and 6.15g) respectively with constant stirring. The resultant suspension was evaporated at 40 °C by rotary evaporator until the dry mass is obtained, washed several time with distilled water, dried overnight at 100 °C and finally calcined at 400 °C for 5 h.

2.4 Characterization of Prepared catalyst

X-ray diffraction (XRD) of sample was carried out using Scintag XDS 2000 diffractometer. Coulter SA 3100 BET surface area and pore volume analyzer using liquid nitrogen at a temperature of (78 K) were used for BET studies. H_2 -TPR and NH_3 -TPD profile was recorded On a TPDRO/1100 Series, Thermo Electron Corporation, Italy. Mettler TGA/SDTA 851e was used for Thermo gravimetric analysis (TGA) of all catalysts. JEOL JSM 6490-A equipped with Energy Dispersive X-ray Spectrometer (EDX) were used for the morphological and compositional characterization of catalysts.

2.5 Catalyst evaluations

As seen in Fig.1 the equipment was made of a stainless steel cell with two windows through which the spectrometer beam can pass. It was connected to a temperature programmer to heat the inside and the windows of the cell. There was a mass flow controller connected to three gas cylinders containing synthesis gas, hydrogen and Argon. The Gas Chromatography was placed at the outlet of the cell and was alimented by helium, air and hydrogen shown in Fig.1.

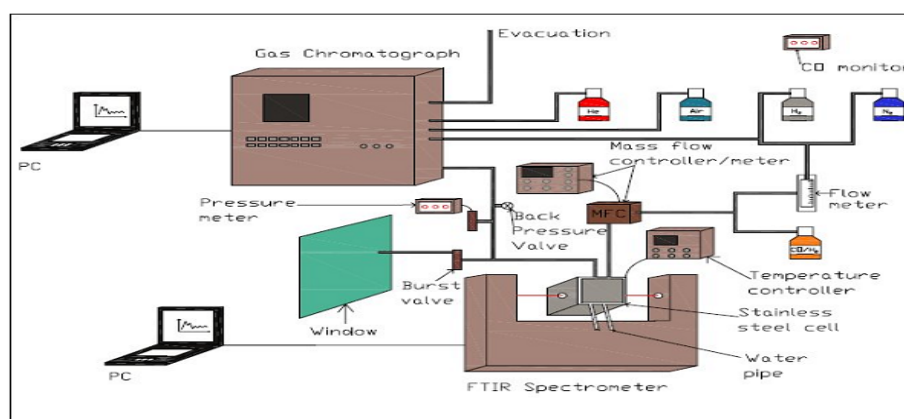


Fig. 1 Schemtic diagram showing the positioning of equipment and flow of gases.

The FT experiments were performed using a sample of catalyst lightly pressed, so as to obtain a disk of 13 mm of diameter with a defined weight; the disk was put into the cell. To remove air from the cell, the experiment begun by flushing Ar at 50 ml/min for 20 min. Once the catalyst had been reduced at 400 °C during 1 h in H_2 , the FTS reaction was carried out at 225, 260, 275 °C at 1,5 and 10 bar pressure and feed flow of synthesis gas during 2-30 h. The synthesis gas was composed of carbon monoxide and hydrogen with a ratio of CO/H_2 (1:2). The products were analyzed on-line by a gas chromatograph (Hewlett-Packard, Model 6890) equipped with flame ionization detector.

3. Results and discussion

3.1 Textural and Structural properties

AlMMT, 10, 15, 20 and 25wt% Co/AlMMT was synthesized and their XRD patterns are given in Fig. 2 and 3.

The naturally occurring MMT was pillared with Al by replacing the small cations such as Ca^{2+} , K^+ and Na^+ present between the electronegative silicate layer of MMT having two dimensional structure by ion exchanged method. The sizes of the interlayer cations give the gallery height of MMT, hence any change in them will surely change the gallery height and d_{001} basal plane [17].

Fig.2 shows the XRD pattern of NaMMT having (001) diffraction peak with a basal spacing of 12.06 Å. Most of the authors agree that the thickness of the host layer of MMT is 9.3 Å [17]. So, the gallery height was found to be 3.3 Å calculated by subtracting the host layer thickness from the obtained basal spacing of the NaMMT.

By observing the XRD spectrum of AlMMT, as shown in Fig.2(b) we find that effect of Al addition has shifted the peak to a comparatively lower theta value and consequently, result an increase of d spacing from 12.06 to 18.7 Å and the gallery height from 3.3 to 9.4 Å. This causes the expansion of the clay interplanar distance with Al pillar, similar to the Keggin type ionic structure $[\text{Al}_{13}\text{O}_4(\text{OH})_{24}(\text{H}_2\text{O})_{12}]^{7+}$ as reported in reference [16]. The XRD spectra of AlMMT give diffraction planes at 8° , 19.7° , 35° and 61.8° which are characteristic of two dimensional layers structure of clay. The intensity of the 001 peak was also decreased which can be attributed to the intercalation of Al into the MMT clay interlayer's. Moreover, no other structural changes were observed in the XRD spectra of both the samples as rest of the peak positions remained unchanged.

Fig.3 shows the XRD pattern of Al MMT catalysts loaded with cobalt. All the catalysts show 001 diffraction peaks and basal reflection of AlMMT with a small decrease in their intensity which corresponds to the slight decrease in layered structure of MMT.

Cobalt loaded catalysts giving cubic cobalt oxides (Co_3O_4) diffraction at 19.5° , 32° , 37° , 45° and 60° (JCPDS 65-3103) indicates a uniform dispersion of pure Co_3O_4 on pillared MMT.

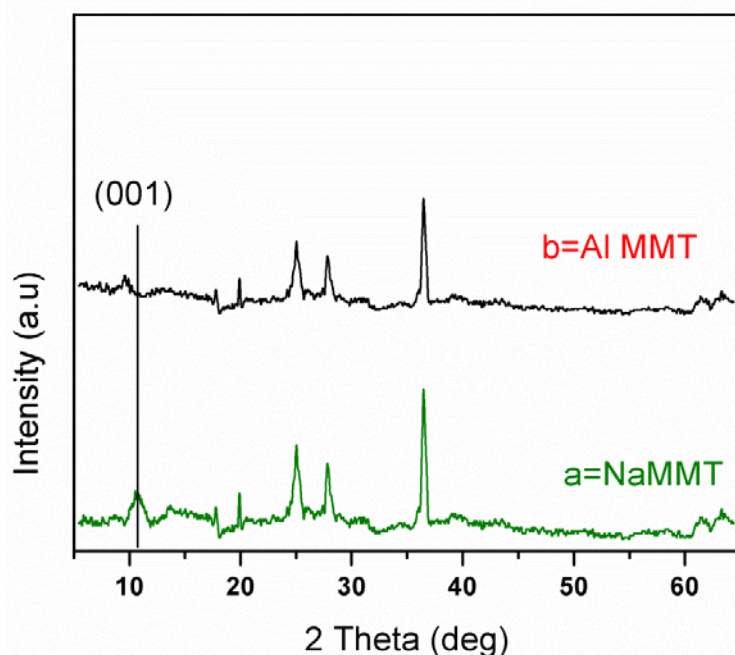


Fig.2 XRD pattern of (a)NaMMT and (b)AlMMT.

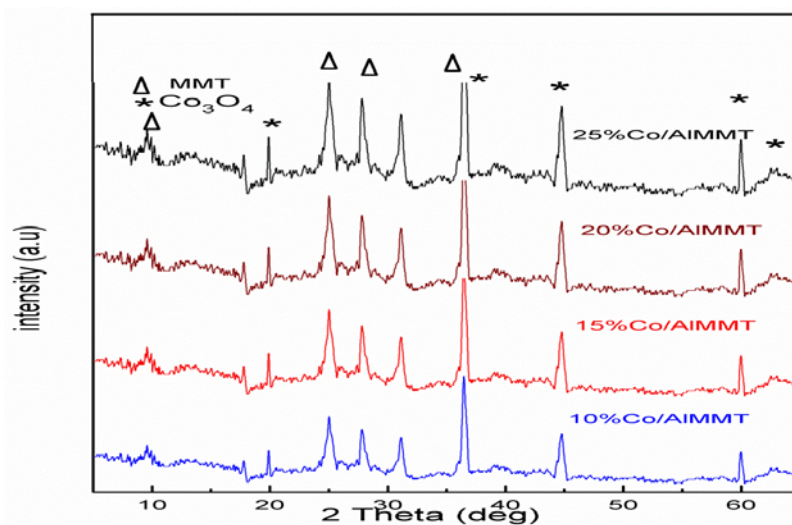


Fig.3 XRD pattern of the 10, 15, 20, 25wt% Co/AlMMT.

Table: 1 Textural property of the prepared catalysts.

Sample	BET (m ² /g)	Pore diameter(Å)	Pore volume(cm ³ /g)
NaMMT	39.24	4.81	0.08
AlMMT	254.00	18.31	0.20
10wt% Co/AlMMT	238.00	15.67	0.18
15wt% Co/AlMMT	235.00	15.35	0.19
20wt% Co/AlMMT	235.00	15.75	0.18
25wt% CO/AlMMT	229.68	15.32	0.19

Table 1 show that NaMMT having lower surface area of 39.243 m²/g while AlMMT having larger surface area of 254 m²/g. The larger surface area of AlMMT is due to the ability of Al to replace the Na⁺ present in MMT results an increase in pore volume responsible for N₂ adsorption [14]. Small decrease in BET surface area for Co-loaded catalysts seen from the table can be attributed to the presence of metal particle at pore opening and on the surface of the pores. The average pore diameter and pore size calculated for all of the sample were constant therefore the pore blocking of Co can be neglected [18]. Enhanced FT activity can be expected from the AlMMT supported Co catalysts due to its high surface area and pore diameter larger than the interlayer distance of MMT similar to the previous study [17]. The adsorption isotherm (Fig.4) for NaMMT shows the non porous nature of NaMMT and the type IV isotherm for Co/Al-MMT confirms its microporous nature. After calcinations at 400 °C the same type isotherm obtained for the all the sample with slight change in pore diameter and pore volume confirmed that the narrow slit shaped porous structure of MMT did not change after calcinations.

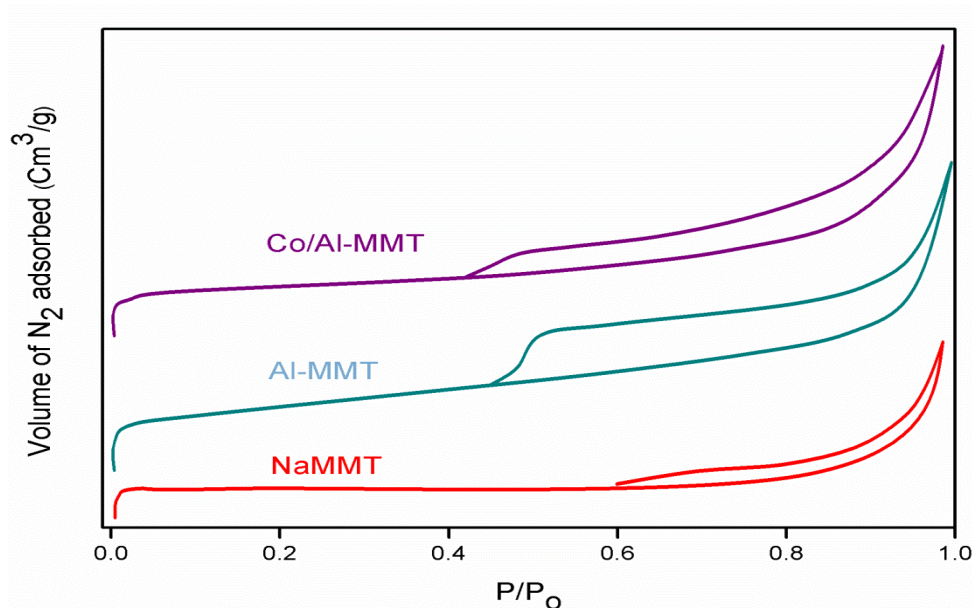


Fig. 4 N_2 Adsorption desorption Isotherm of Na MMT, AlMMT and Co/Al-MMT catalysts.

3.2. Acidic Property

NH_3 -TPD was used to evaluate the acidic properties of the prepared samples (Fig.5). It is reported that pillared clay poses both Lewis and Bronsted acidic site [19]. The NH_3 -TPD profile showed that the samples possess both weaker acidic sites desorption peak at 150 °C and stronger Lewis acidic sites desorption at 600 °C. The weak Bronsted acidic sites give the lower temperature NH_3 desorption peak while the high temperature desorption of NH_3 occurs due to the strong Lewis acidic sites [20]. The Co loading shows little effect on the acidity of pillared MMT by increasing the intensity of Bronsted acid peak hence improving the Bronsted acidity. The overall acidic property of the Co loaded sample slightly decreases, may be as a result of Co deposition on pore opening and blockage of some pore responsible for NH_3 desorption and hence decreases the density of Lewis acidic sites of pillared clay similar result have already been reported for vanadium loaded pillared clay [19].

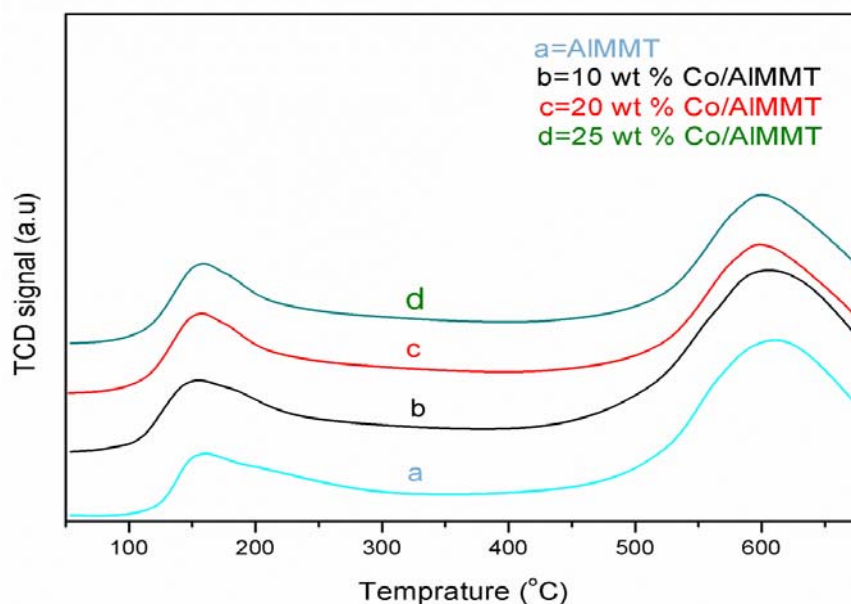


Fig. 5 NH_3 -TPD profile of Samples.

3.3 SEM Studies

To study the surface morphology of our prepared sample SEM characterization was used. The SEM micrograph for NaMMT and Co/AlMMT are given in Fig.6a and b showed the same flake like morphology which infer that the calcinations temperature, pillaring of Al and Co loading have no effect on the MMT layered structure.

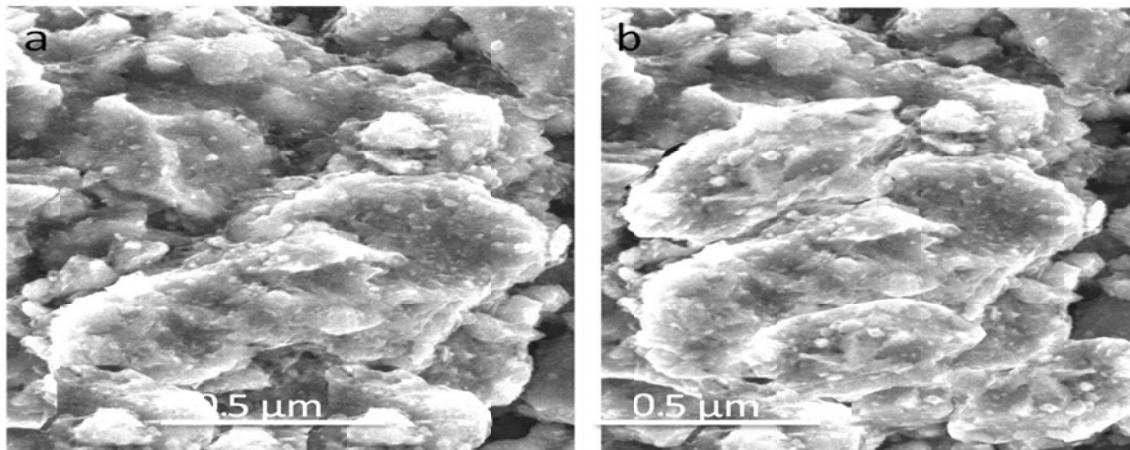


Fig. 6 SEM Images of (a)NaMMT(b) Co/AlMMT

3.4 Reduction behavior

The H_2 -TPR profile of 10%, 15 % and 20% and 25% Co/AlMMT are given in Fig.7. The small peak around 210 °C for the sample is due to the decomposition of $Co(NO_3)_2$ remain in the sample after calcinations, while the first and second reduction peak for 20% Co/NaMMT at 278 and 379 °C is due to the reduction of Co_3O_4 to CoO and CoO to metallic Co respectively is similar to the previously reported results [14]. The TPR profile of AlMMT supported Co samples shows that the two steps reduction of cobalt oxides occurs at lower temperature of 268 °C and 365 °C respectively. The decrease in reduction temperature of AlMMT supported cobalt samples can be attributed to enhanced dispersion of cobalt particles on the surface of support and high surface area of pillared montmorillonite as results of Al-pillaring.

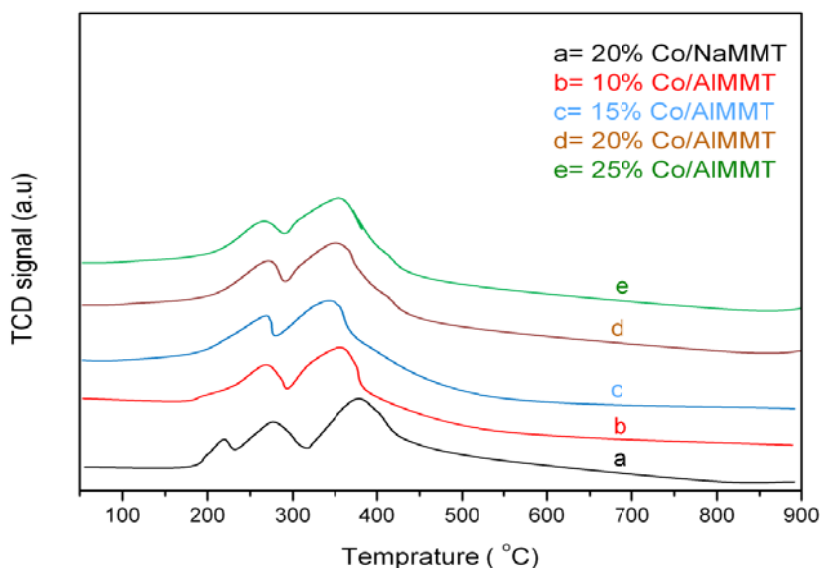


Fig. 7 H_2 -TPR profile of the prepared samples.

3.5 Thermogravimetric analysis (TGA)

TGA of 20wt% Co/NaMMT and different wt% Co/AlMMT has been carried out (Fig.8). This is clearly seen from TGA data that all samples exhibit continuous weight loss behavior till 800 °C. The weight loss upto 160 °C can be attributed to the removal of surface adsorbed water while the weight loss between 160 °C to 500 °C is attributed to the interlayer water and due to the dehydroxylation of the clay. Interestingly, as the wt% of Co increased, the weight losses around 300 °C also increased. The continuous weight loss from 600 °C till 800 °C was attributable to the removal of hydroxide groups as a result of dehydroxylation of pillar and clay structure, causing collapse in MMT layer structure [19-23]. These results also show an agreement with previously reported results for thermal behavior of vanadia-loaded pillared clays [21].

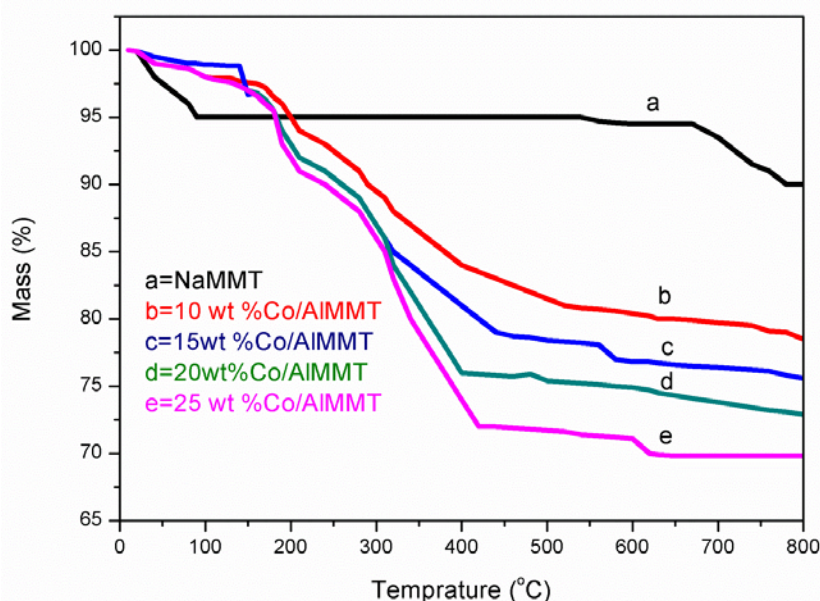


Fig. 8 TGA Curve of the samples.

4. FT catalytic activity test

4.1 Catalytic activity of 20wt% Co/NaMMT

The catalytic performance of 20wt% Co/NaMMT in terms of selectivity, CO-conversion and time on stream is presented in Fig. 9 (a) with increasing time on stream (TOS), the catalysts show increased CH₄ selectivity and very small selectivity for the remaining hydrocarbons. The catalytic stability of Co/NaMMT was studied for 10 h and we initially observed a CO-conversion of around 10% but it went on decreasing till it reached to less than 5% in 10 h TOS. Simultaneously, increase in the CO₂ and CH₄ selectivity of catalysts was observed which increased to more than 40% during this TOS. These gases are the most unwanted products in FT synthesis and must be reduced to the minimum possible levels. The low FT activity of the Co/NaMMT observed in this case can be attributed to their lower surface area, larger particle size of Co over NaMMT and hindrance of CoO reduction to Co by NaMMT as reported in reference [24]. From this study, it was found that first two had no significant effect on the CO-conversion but the lower FT activity and higher selectivity toward CH₄ was mainly due the incomplete reduction of cobalt oxides. Beside this, the presence of alkali and alkaline earth metals specially Na showed marked negative effect on activity of FT catalysts due to the inhibition of CoO reduction [14].

The FT products obtained at a TOS of 10 h for this catalyst mainly include the C₂-C₄ and lesser amount of C₅-C₇ hydrocarbons. From the above discussions, it can be concluded that Co/NaMMT shows very poor catalytic activity in FT synthesis.

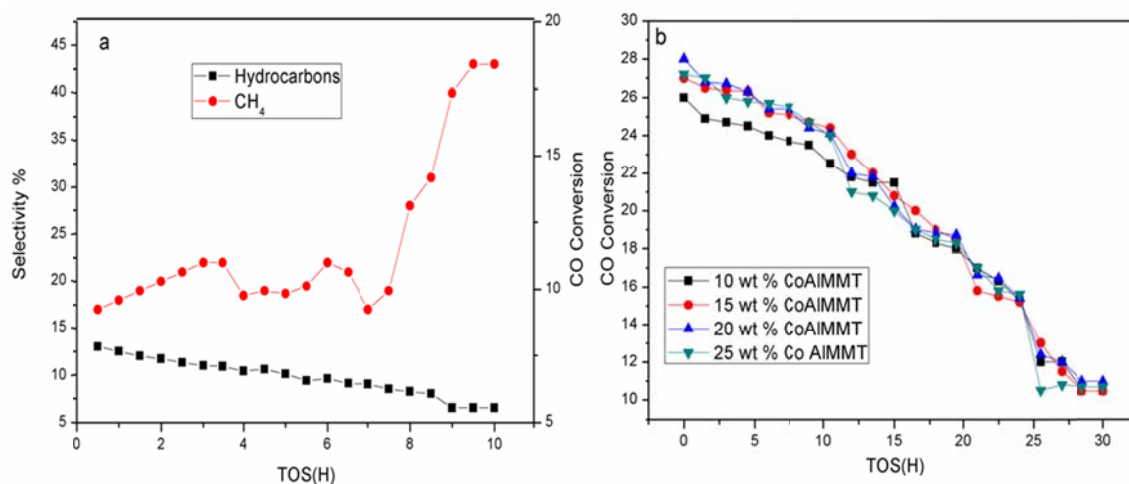


Fig. 9 CO-conversion and methane selectivity versus Time on stream for (a) 20% Co/NaMMT, (b) Different wt% Co/AlMMT catalysts.

4.2 Catalytic activity of Al pillared MMT (Different wt% Co/AlMMT)

The pillaring of NaMMT with Al enhances the surface area of support MMT from 39.243 to 254 m²/g. It also increases the pore volume and pore diameter due to the contribution of Al to replace the Na⁺ in the MMT interlayer [14] and hence the catalytic activity of Co/MMT catalysts. The inter layer cation plays a vital role in the CO-conversion. As compared to Co supported on Na MMT, Al-pillared MMT supported catalysts show higher CO-conversion. The CO-conversion was 26, 27, 28 and 27.2% for 10, 15, 20 and 25wt% Co/AlMMT catalysts respectively (Fig.9b) which decreases with TOS and reaches a minimum of 10.5% after 30 h of TOS. The higher CO-conversion was seen for 20wt% Co/AlMMT catalysts which was 28 %, decreases with TOS and reaches a minimum of 11% after 30 h of TOS. The CO-conversion in case of AlMMT supported Co catalysts was higher than NaMMT supported catalysts, indicating that the Al-pillaring of MMT has a positive impact on the CO-conversion in FT synthesis was alike to the results obtained by Wang et al [14]. The FT products obtained (Table 2) over Co/AlMMT catalyst showed improved selectivity of C₂-C₁₂ hydrocarbons and decreased selectivity towards higher molecular weight hydrocarbons C₂₁ at a TOS of 2- 30 h. This decrease in C₂₁ selectivity is due to the cracking of long chain hydrocarbons at the acidic site of MMT [25-29]. The selectivity towards C₂-C₁₂ hydrocarbons was found maximum at a TOS of 8 h.

Table 2 Results of Different catalysts for FT synthesis

Catalysts	CO-conversion	CO ₂	C ₁ (wt%)	C ₂ -C ₁₂ (wt%)	C ₁₃ -C ₂₀ (wt%)	C ₂₁ (wt%)
Selectivity						
20wt% Co/NaMMT	10.2	2.3	40.1	12.5	8.2	37.4
20wt% Co/AlMMT	28.3	2.5	27.2	18.2	11.2	41.4
10wt% Co/AlMMT	26.5	2.0	26.0	19.2	11.7	41.1
15wt% Co/AlMMT	27.0	1.9	26.8	20.0	12.1	39.0
25wt% Co/AlMMT	27.2	1.8	28.3	19.0	13.1	37.7

4.3 Effect of reaction temperature on catalytic activity of catalysts.

The effect of reaction temperature on catalytic activity of 20wt% Co/AlMMT was investigated (Fig.10 a). The reaction carried out at a temperature of 225 °C gives almost 28 % CO-conversion with methane selectivity of 27.2%. When the reaction temperature is increased to 260 and 275 °C the CO-conversion and methane selectivity were also increased to 32, 35 and 37, 40% respectively along with decrease in C₅₊ hydrocarbons selectivity. This effect of the catalysts can be attributed to the high hydrogenation activity of catalysts at high temperature similar to the performance of standard cobalt thorium catalysts [30]. Increase in reaction temperature from 225 to 275 °C produces too much methane and therefore it is not beneficial in Co based FT synthesis as an agreement with the results reported earlier [31].

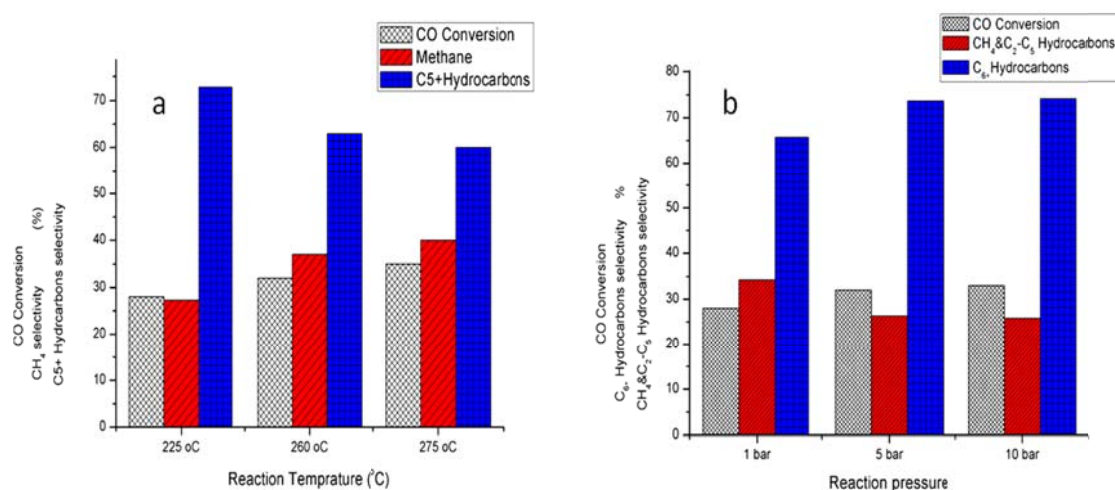


Fig. 10 Effect of reaction temperature (a) and reaction pressure (b) on FT catalytic activity.

4.4 Effect of reaction pressure on catalytic activity of catalysts.

Reaction pressure largely effect the activity and selectivity of FT catalysts. The FT reaction carried out at a pressure of 1, 5 and 10 bar showed CO-conversion of 28, 32 and 33% respectively (Fig.10b). The selectivity of C₆₊ hydrocarbons increased and that of methane and C₂-C₅ hydrocarbons decreases with increase in pressure. High pressure favors the production of high molecular weight hydrocarbons as a result of chain growth probability which normally increased with increasing pressure as reported earlier [32]. The increase in CO-conversion is due to the increase in partial pressure of hydrogen and the increase selectivity of the C₆₊ hydrocarbons is due

to the increase CO partial pressure while the reaction rate in such type of reaction is proportional to the hydrogen partial pressure as reported previously [33].

5. Conclusions

The ability of MMT as a support for FT catalysts was successfully improved by pillaring with Al. The inhibition of CoO reduction and increased methane selectivity of MMT in FT reaction caused by the presence of Na in MMT was overcome by pillaring with Al. Increase in the surface area from 39.243 to 254 m²/g along with increase in pore volume and pore diameter may be explained due to the contribution of Al to replace the Na⁺ in the MMT results into its pore opening and production of new pores responsible for N₂ adsorption [14].

The aptitude of Co catalysts for FT synthesis was improved by supporting it on AlMMT. AlMMT supported Co catalysts showed higher CO-conversion and greater selectivity towards C₂-C₁₂ hydrocarbons and decreases selectivity towards C₂₀₊ hydrocarbons as a result of hydrocracking reaction taking place at the acidic sites of montmorillonite. With increase in reaction temperature methane selectivity and CO-conversion increased and the selectivity towards C₅₊ hydrocarbons decreased due to the high hydrogenation activity of catalysts at high temperature. Decrease in methane selectivity while increase in C₅₊ hydrocarbons and CO-conversion was observed when the pressure was increased to 5 and 10 bar.

Acknowledgements

The author would like to thank Higher Education Commission of Pakistan for the financial support of this work under Indigenous-5000 PhD Fellowship program.

References

- [1] H. Schulz, *Appl. Catal. A*, **186** 3 (1999).
- [2] J.J.H.M. Font Freide, T.D. Gamlin, C. Graham, J.R. Hensman, B. Nay, C. Sharp, *Top. Catal.* **26**, 3 (2003).
- [3] M.E. Dry, *Catal. Today*. **71** 227 (2002).
- [4] A.Y. Khodakov, W. Chu, P. Fongarland, *Chem. Rev.* **107** 1692 (2007).
- [5] H. Wang, Y. Yang, J. Xu, H. Wang, M. Ding, Y. Li, *J. Mol. Catal. A: Chem* **326** 29 (2010).
- [6] S. Li, S. Krishnamoorthy, A. Li, G.D. Meitzner, E. Iglesia, *J. Catal.* **206** 202 (2002).
- [7] A. Dinse, M. Aigner, M. Ulbrich, G.R. Johnson, A.T. Bell, *J. Catal.* **288** 104 (2012).
- [8] S.T. Hussain, M. Mazhar, M.A. Nadeem, *J. Nat. Gas Chem.* **18** 187 (2009).
- [9] H. Li, S. Wang, F. Ling, J. Li, *J. Mol. Catal. A: Chem.* **244** 33 (2006).
- [10] J. Panpranot, J.G. Goodwin Jr, A. Sayari, *J. Catal.* **211** 530 (2002).
- [11] G. Jacobs, T.K. Das, Y. Zhang, J. Li, G. Racoillet, B.H. Davis, *Appl. Catal. A*. **233** 263 (2002).
- [12] H. Xiong, Y. Zhang, K. Liew, J. Li, *J. Mol. Catal. A: Chem.* **295** 68 (2008).
- [13] G. Prieto, A. Martínez, R. Murciano, M.A. Arribas, *Appl. Catal., A*. **367** 146 (2009).
- [14] G.-W. Wang, Q.-Q. Hao, Z.-T. Liu, Z.-W. Liu, *Appl. Catal., A*. **405** 45 (2011).
- [15] R. Issaadi, F. Garin, C.E. Chitour, G. Maire, *Appl. Catal. A*. **207** 323 (2001).
- [16] Martí, amp, x, M.J. nez-Ortiz, G. Fetter, Domi, J.M. nguez, J.A. Melo-Banda, R. Ramos-Gómez, *Microporous and Mesoporous Mater.* **58** 73 (2003).
- [17] Y. Liu, K. Murata, K. Okabe, M. Inaba, I. Takahara, T. Hanaoka, K. Sakanishi, *Top. Catal.* **52**, 597 (2009).
- [18] H. Su, S. Zeng, H. Dong, Y. Du, Y. Zhang, R. Hu, *Appl. Clay Sci.* **46** 325 (2009).
- [19] K.V. Bineesh, D.-K. Kim, M.-I.L. Kim, D.-W. Park, *Appl. Clay Sci.* **53** 204 (2011).
- [20] K.V. Bineesh, S.-Y. Kim, B.R. Jermy, D.-W. Park, *J. Ind. Eng. Chem.* **15** 207 (2009).
- [21] K.V. Bineesh, D.-K. Kim, D.-W. Kim, H.-J. Cho, D.-W. Park, *Energy Environ. Sci.* **3**, 302 (2010).

- [22] P. Cañizares, J.L. Valverde, M.R. Sun Kou, C.B. Molina, *Microporous and Mesoporous Mater.* **29** 267 (1999).
- [23] K.V. Bineesh, D.-K. Kim, H.-J. Cho, D.-W. Park, *J. Ind. Eng. Chem.* **16** 593 (2010).
- [24] J. Thiessen, A. Rose, J. Meyer, A. Jess, D. Curulla-Ferré, *Microporous and Mesoporous Mater.* **164** 199 (2012).
- [25] S.-H. Kang, J.-H. Ryu, J.-H. Kim, P.S. Sai Prasad, J.W. Bae, J.-Y. Cheon, K.-W. Jun, *Catal. Lett.* **141** 1464 (2011).
- [26] C. Ngamcharussrivichai, A. Imyim, X. Li, K. Fujimoto, *Ind. Eng. Res.* **46** 6883 (2007).
- [27] A.K. Dalai, B.H. Davis, *Appl. Catal., A*: **348** 1 (2008).
- [28] J. Bao, J. He, Y. Zhang, Y. Yoneyama, N. Tsubaki, *Angewandte Chemie International Edition* **47**, 353 (2008).
- [29] Z.W. Liu, X.H. Li, K. Asami, K. Fujimoto, *Catal. Today*. **104** 41 (2005).
- [30] S. Colley, R.G. Copperthwaite, G.J. Hutchings, M. Van der Riet, *Ind. Eng. Res.* **27**, 1339 (1988).
- [31] D. Das, G. Ravichandran, D.K. Chakrabarty, *Appl. Catal., A*: **131** 335 (1995).
- [32] Z. Yan, Z. Wang, D.B. Bukur, D.W. Goodman, *J. Catal.* **268** 196 (2009).
- [33] H. Schulz, M. Claeys, *Appl. Catal., A*: **186** 91 (1999).